STRESS-STRAIN MODEL FOR PARTIAL CFRP CONFINED CONCRETE

Débora R.S.M. Ferreira[*] and Joaquim A. O. Barros[+]

[*] PhD student, Dept. of Civil Engineering,
Universidade of Minho, Campus de Azurém,
4810-058 Guimarães, Portugal.
E-mail: debora@ipb.pt

[+] Associate Professor, Dept. of Civil Engineering,
Univ. of Minho, Campus de Azurém,
4810-058 Guimarães, Portugal.
E-mail: barros@civil.uminho.pt

Keywords: Carbon Fiber Reinforced Polymers, Confinement, Concrete, Columns, Confinement model.

Summary: *Concrete columns requiring strengthening intervention always contain a certain percentage of steel hoops. Applying strips of wet lay-up carbon fiber reinforced polymer (CFRP) sheets in-between the existent steel hoops might, therefore, be an appropriate confinement technique with both technical and economic advantages, when full wrapping of a concrete column is taken as a basis of comparison.*

To assess the effectiveness of the partial wrapping technique, circular cross section concrete columns were confined by distinct CFRP arrangements and tested under direct compression. The experimental program was designed to evaluate the influence of the concrete strength class, the stiffness of the wet lay-up CFRP sheet, the distance between strips, the width of the strip, and the number of layers per each strip.

The Harajli et al. model was modified in order to predict the compression stress-strain behaviour of reinforced concrete column elements partially and totally confined by CFRP lay-up sheets. The main results of the experimental program are hereby presented and analysed. The model's performance is assessed using the experimental results.

1 INTRODUCTION

Reinforcement concrete columns can be strengthened by a carbon fiber reinforced polymer (CFRP) jacket, which provides lateral confinement to the column. Applying strips of wet lay-up CFRP sheets in-between the existing steel hoops might, therefore, be an appropriate confinement technique with both technical and economic advantages, when full wrapping of a concrete column is taken as a basis of comparison.

Analytical models have been proposed to simulate the stress-strain compression response of full FRP-wrapped concrete elements [1-5]. The applicability of these models to predict the behaviour of concrete columns confined by discrete CFRP arrangements is still limited.

In the present work, the principles proposed by Harajli *et al.*, were used to develop a confinement model to simulate, not only full wrapped specimens but also those with discrete arrangements. The performance of the model was appraised using results obtained in the experimental program carried out.

2 EXPERIMENTAL PROGRAM AND CONFINEMENT ARRANGEMENTS

The experimental program deals with direct compression tests with reinforced concrete (RC) column elements of 600 mm high and 200 mm diameter. This program is composed by several groups of tests in order to evaluate the influence of the following parameters on the load carrying and deformation capacity of RC elements submitted, predominantly, to compression loading: concrete strength class (two compressive strengths, 16MPa and 32MPa ,were selected); stiffness of the CFRP-based confinement system (two CFRP sheets were used, one of 300 g/m^2 of fibers and the other of 200 g/m^2 of fibers); width (W) and spacing (s') of the CFRP strips; number of CFRP layers per strip (L); percentage of the longitudinal, ρ_{sl} , and transversal, ρ_{st} , steel reinforcement ratio. Due to lack of space, only the groups of tests C16S200Φ8, C16S300Φ8, C32S200Φ8 and C32S300Φ8, indicated in Table 1, are analyzed in the present paper.

Table1 – Experimental program

<table>
<tr>
<td> 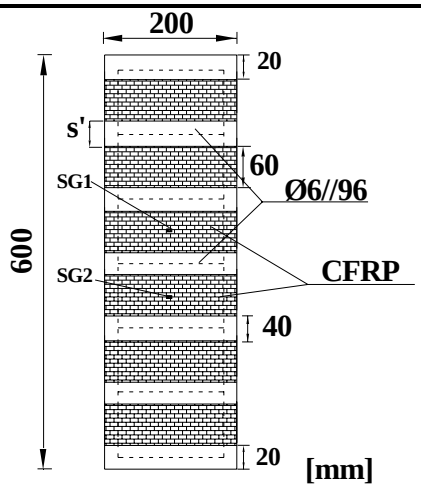
</td>
<td colspan="2"> 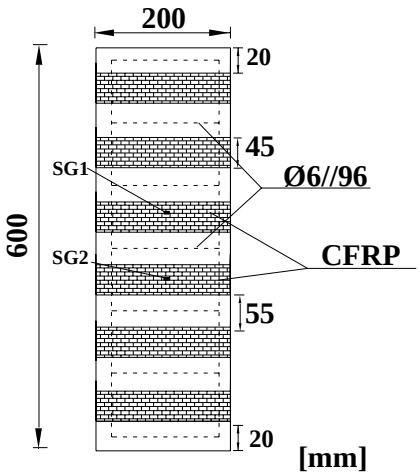
</td>
<td colspan="2"> 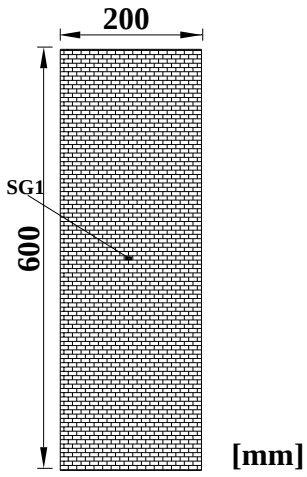
</td>
</tr>
<tr><td>W [mm]</td><td>Designation</td><td>s’ [mm]</td><td>W [mm]</td><td>Designation</td></tr>
<tr><td rowspan="2">45</td><td>W45S6L3</td><td rowspan="2">55</td><td rowspan="4">600</td><td rowspan="2">W600S1L3</td></tr>
<tr><td>W45S6L5</td></tr>
<tr><td rowspan="2">60</td><td>W60S6L3</td><td rowspan="2">40</td><td rowspan="2">W600S1L5</td></tr>
<tr><td>W60S6L5</td></tr>
<tr><td colspan="5">Concrete strength class: C16/20 and C30/35</td></tr>
<tr><td colspan="5">Longitudinal bars: $\phi 8$</td></tr>
<tr><td rowspan="2">Type of CFRP sheet</td><td colspan="2">CF130 S&P 240 (300 gm/m^2)</td><td rowspan="2">Group of test series</td><td>C16S300$\phi 8$
C32S300$\phi 8$</td></tr>
<tr><td colspan="2">CF120 S&P 240 (200 gm/m^2)</td><td>C16S200$\phi 8$
C32S200$\phi 8$</td></tr>
</table>

The confinement systems are composed by strips of CFRP sheet bonded to concrete and to subjacent layers by epoxy resin. Each specimen is designated by W*i*S*j*L*k,* where W*i* is the strip width, S*j* is the number of strips along the specimen and L*k* is the number of CFRP layers per each strip. In the adopted designation for a group of test series, the C16 and C32 designation indicates that concrete specimens with an average compressive strength of 16 and 32 MPa, respectively, while S200 and S300 denote the type of CFRP sheet, 200 g/m^2 and 300 g/m^2, respectively. Finally, $\Phi 8$ indicates the diameter, in mm, of the longitudinal steel bars.

As Figure 1 shows, the partially-wrapped specimens are confined by six strips (W45S6 and W60S6). These three test series have two sub-series, one of three layers per strip (L3) and another with five layers per strip (L5).


W45S6

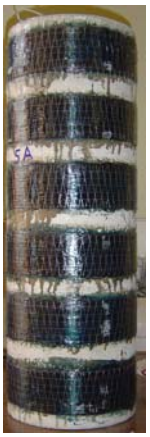
W60S6


W600S1

Figure 1 : Confinement arrangements

3 EXPERIMENTAL RESULTS

Tables 2 and 3 include the main effectiveness indicators provided by the applied confinement systems. In these tables, $f_{co,UPC}$ is the compressive strength of unconfined plain concrete specimens (UPC), $f_{co,URC}$ is the compressive strength of unconfined reinforced concrete specimens, $\varepsilon_{co,UPC}$ is the specimen axial strain corresponding to $f_{co,UPC}$ and $\varepsilon_{co,UPC}$ is the specimen axial strain corresponding to $f_{co,URC}$. Each value in Tables 2 and 3 is the average of results obtained in the two specimens of each series. In specimens W600S1L5 of C32S200ϕ8 and in specimens W60S6L5, W600S1L3 and W600S1L5 of C32S300ϕ8 series (fully wrapped specimens) the maximum load carrying capacity of the equipment was attained without failure of these specimens. The values indicated in Table 3 correspond to the end of this test phase. Since the load carrying capacity of the equipment can be doubled if the tests are carried out in a non-closed loop control, the specimens of these series were again tested up to their failure, and the attained f_{cc} values are indicated in Table 3 within square brackets. As it was impossible to record strains in the CFRP during this second loading phase of these tests, only the compressive strength was recorded.

Results of Table 2 indicate that, in C16S200ϕ8, $f_{cc}/f_{co,URC}$ varied from 1.9 in series confined with strips of 45 mm width and three layers per strip (W45S5L3), ρ_f=0.31%, up to 4.2 in the fully-wrapped series with five layers, ρ_f=1.13%. For C16S300ϕ8 these limit values increased to 2.5 and 5.1, respectively, since the CFRP confinement ratio increased due to the higher thickness of the CF130 sheet (from ρ_f=0.48% up to ρ_f=1.76%). Table 3 shows that, in the case of C32S200ϕ8, $f_{cc}/f_{co,URC}$ varied from 1.37 for ρ_f=0.31% up to 2.99 for ρ_f=1.13%, while for C32S300ϕ8 the values were in the range 1.60 to 3.27 for ρ_f=0.48% and ρ_f =1.76%, respectively. In terms of $\varepsilon_{cc}/\varepsilon_{co,URC}$, the values ranged from 4.8 up to 10.5 for C16S200ϕ8 series, 7.3 up to 14.8 for C16S300ϕ8, 3.1 up to 6.1 for C32S200ϕ8 and 4.0 up to 7.5 for C32S300ϕ8. However, the upper bound values of the ranges of $\varepsilon_{cc}/\varepsilon_{co,URC}$ for these last two series of tests would have been greater if the strains in the CFRP of the specimens, that have not failed in the closed loop control test phase, had been recorded in the non-closed loop control phase. In all series of tests, the increase of $\varepsilon_{cc}/\varepsilon_{co,URC}$ ratio with ρ_f was more pronounced in specimens of discrete confinement arrangements than in fully-wrapped specimens. The plastic deformation of the concrete in-between the CFRP strips may justify this occurrence.

The last column of Tables 2 and 3 shows that, at specimen failure always occurring by the CFRP tensile rupture, the maximum tensile strain in the direction of the fibers, ε_{fmax}, varied from 27% up to 88% of the CFRP ultimate tensile strain, $\varepsilon_{fu.}$ These values are only for specimens that failed when the equipment was working in closed-loop control. As Lam and Teng (2003) have already reported, the variation of the strain field in the CFRP depends considerably on the distribution of the damage in the concrete specimen. Taking this into account and considering that only one or two strain gauges were applied per specimen for recording the CFRP strain variation, it is not surprising that a tendency was not determined for the $\varepsilon_{fmax}/\varepsilon_{fu}$ ratio. A high scatter was registered on the maximum strain values in the CFRP, since the recorded values only represent the areas where the strain gauges were placed. Hence, these values are too dependent on the specimen failure mode configuration.

Table 2. Main indicators of the efficacy of the confinement systems in the C16S200ϕ8 and C16S300ϕ8 test series.

Type of sheet	Specimen designation	L	ρ_f (%)	f_{cc} (MPa)	ε_{cc} (%)	$f_{cc}/f_{co,URC}$	$\varepsilon_{cc}/\varepsilon_{co,URC}$	ε_{fmax} (%)	$\varepsilon_{fmax}/\varepsilon_{fu}$
	Unconf. plain concrete (UPC)			13.87 ($f_{co,UPC}$)	0.003 ($\varepsilon_{co,UPC}$)	-	-	-	-
	Unconf. Reinf. Conc. (URC)			14.71 ($f_{co,URC}$)	0.004 ($\varepsilon_{co,URC}$)	-	-	-	-
C16S200ϕ8	W45S6L3	3	0.31	27.68	0.019	1.88	4.75	0.0069 (SG1)	0.44 (SG1)
								0.0083 (SG2)	0.53 (SG2)
C16S300ϕ8			0.48	36.04	0.034	2.45	7.25	0.00846 (SG1)	0.55 (SG1)
								0.0103 (SG2)	0.65 (SG2)
C16S200ϕ8	W45S6L5	5	0.51	35.50	0.030	2.41	7.50	0.0089 (SG1)	0.57 (SG1)
								0.0073 (SG2)	0.47 (SG2)
C16S300ϕ8			0.80	45.82	0.047	3.11	11.75	0.00934 (SG1)	0.60 (SG1)
								0.00828 (SG2)	0.53 (SG2)
C16S200ϕ8	W60S6L3	3	0.41	34.36	0.022	2.34	5.50	0.0078 (SG1)	0.51 (SG1)
								0.0066 (SG2)	0.42 (SG2)
C16S300ϕ8			0.64	46.13	0.037	3.14	9.25	0.0126 (SG1)	0.82 (SG1)
								0.0120 (SG2)	0.78 (SG2)
C16S200ϕ8	W60S6L5	5	0.68	43.53	0.035	2.96	8.75	0.0092 (SG1)	0.59 (SG1)
								0.0060 (SG2)	0.44 (SG2)
C16S300ϕ8			1.06	64.96	0.059	4.42	14.75	0.0137 (SG1)	0.88 (SG1)
								0.0122 (SG2)	0.79 (SG2)
C16S200ϕ8	W600S1L3	3	0.68	47.93	0.032	3.26	8.00	0.0098 (SG1)	0.63 (SG1)
C16S300ϕ8			1.06	52.19	0.033	3.55	8.25	0.00769 (SG1)	0.50 (SG1)
C16S200ϕ8	W600S1L5	5	1.13	61.98	0.042	4.21	10.5	0.010 (SG1)	0.65 (SG1)
C16S300ϕ8			1.76	75.18	0.050	5.11	12.50	0.00757 (SG1)	0.49 (SG1)

Table 3. Main indicators of the efficacy of the confinement systems in the C32S200ϕ8 and C32S300ϕ8̃ test series.

Type of sheet	Specimen designation	L	ρ_f (%)	f_{cc} (MPa)	ε_{cc} (%)	$f_{cc}/f_{co,URC}$	$\varepsilon_{cc}/\varepsilon_{co,URC}$	ε_{fmax} (%)	$\varepsilon_{fmax}/\varepsilon_{fu}$
	Unconf. plain concrete (UPC)			30.31 ($f_{co,UPC}$)	0.003 ($\varepsilon_{co,UPC}$)	-	-	-	-
	Unconf. Reinf. Conc. (URC)			32.80 ($f_{co,URC}$)	0.003 ($\varepsilon_{co,URC}$)	-	-	-	-
C32S200ϕ8	W45S6L3	3	0.31	44.80	0.0092	1.37	3.07	0.00867 (SG1)	0.56 (SG1)
								0.00422 (SG2)	0.27 (SG2)
C32S300ϕ8			0.48	52.76	0.0132	1.60	4.40	0.00743 (SG1)	0.47 (SG1)
								0.00585 (SG2)	0.38 (SG2)
C32S200ϕ8	W45S6L5	5	0.51	55.36	0.0139	1.69	4.63	0.00702 (SG1)	0.45 (SG1)
								0.00672 (SG2)	0.43 (SG2)
C32S300ϕ8			0.80	60.70	0.0185	1.85	6.17	0.00883 (SG1)	0.57 (SG1)
								0.00796 (SG2)	0.51 (SG2)
C32S200ϕ8	W60S6L3	3	0.41	54.37	0.0137	1.66	4.57	0.00731 (SG1)	0.47 (SG1)
								0.00822 (SG2)	0.53 (SG2)
C32S300ϕ8			0.63	63.50	0.0185	1.94	6.17	0.00689 (SG3)	0.44 (SG1)
								0.00711 (SG4)	0.46 (SG2)
C32S200ϕ8	W60S6L5	5	0.68	67.09	0.0179	2.05	5.97	0.00721 (SG1)	0.47 (SG1)
								0.00804 (SG2)	0.52 (SG2)
C32S300ϕ8			1.06	71.52* 84.44**	0.0225	2.18* 2.57**	7.50	0.00902 (SG1)	0.58 (SG1)
								0.00764 (SG2)	0.49 (SG2)
C32S200ϕ8	W600S1L3	3	0.68	71.37	0.0181	2.17	6.03	0.0131 (SG1)	0.85 (SG1)
C32S300ϕ8*			1.06	71.56* 93.59**	0.0168	2.18* 2.86**	5.60	0.00718 (SG1)	0.46 (SG1)
C32S200ϕ8*	W600S1L5	5	1.13	71.51* 98.36**	0.014*	2.18* 2.99**	4.67	0.00735 (SG1)	0.47 (SG1)
C32S300ϕ8*			1.76	71.88* 111.1**	0.0121	2.19* 3.27**	4.03	0.00188 (SG1)	0.12 (SG1)

* Values recorded when the load carrying capacity of the equipment was attained, without the occurrence of the failure of the specimens

** Values at the failure of the specimen

4 THE MODEL

Although several confinement models have been proposed to simulate the stress-strain compression response of full FRP-wrapped concrete elements [1-5], there is a dearth of models able to accurately predict the behaviour of concrete columns confined by discrete CFRP arrangements. In the present work, the principles proposed by Harajli *et al.* (2006) were used to develop a confinement model to simulate, not only full wrapped specimens but also those confined with discrete arrangements.

The model, herein proposed, is based on the two stress-strain branches schematically represented in Figure 2. Point A, characterized by an ε_{cA} strain and an f_{cA} stress, separates the domain between a marginal and a significant influence of the effective lateral confining pressure, provided by the CFRP confinement arrangements, f_{fl}. Since the concrete volumetric expansion starts to occur before the compressive strength of unconfined concrete specimens, point A is evaluated upon a certain minimum value of the CFRP strain, ε_f.

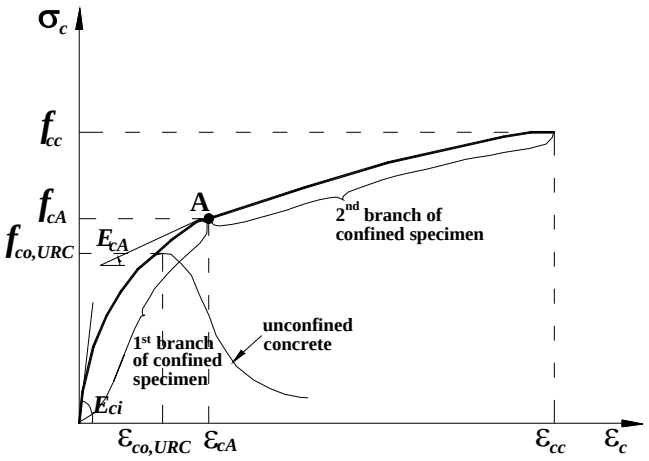

Figure 2: Schematic representation of the stress-strain model for CFRP confined concrete

Based on the strains measured in the CFRP at the specimen axial level corresponding to $\varepsilon_{co,URC}$ (strain at the compressive strength of unconfined reinforced concrete column, URC) a value of about 3.0×10^{-5} was assumed for ε_f to define ε_{cA} and f_{cA}. To obtain ε_{cA} and f_{cA}, as well as the σ_c-ε_c points that define the second branch, the following equations are used [5]:

$$\sigma_c = f_{co,URC} + k_1 \, f_l \text{ for } \varepsilon_c \geq \varepsilon_{cA} \tag{1}$$

$$\varepsilon_c = \varepsilon_{co,URC} \left[1 + k_2 \left(\frac{\sigma_c}{f_{co,URC}} - 1 \right) \right] \text{ for } \varepsilon_c \geq \varepsilon_{cA} \tag{2}$$

where

$$f_l = f_{fl} + f_{sl} \frac{A_{cc}}{A_g} \tag{3}$$

is the effective lateral confinement pressure, and k_1 and k_2 are two parameters that are obtained from the experimental results, [6]. In Eq. (4) and (5) f_{fl} and f_{sl} represent the effective lateral confining

pressure exerted by CFRP and ordinary steel hoops, respectively, and can be determined from the following equations:

$$f_{fl} = \frac{\alpha_{fe}\ \alpha_{fv}\ \rho_f\ E_f}{2}\ \varepsilon_f \tag{4}$$

$$f_{sl} = \frac{\alpha_{se}\ \alpha_{sv}\ \rho_{st}}{2}\ f_{syt} \tag{5}$$

where ρ_f is the CFRP volumetric ratio, E_f is the CFRP elasticity modulus, ρ_{st} is the volumetric ratio of steel hoops (Mander *et al.* 1988), α_{fe} and α_{fv} are the coefficients that account for the effectiveness of the FRP systems in the confinement of the concrete along the specimen cross section's plane, and the concrete between steel hoops, respectively [7]:

$$\alpha_{fv} = \frac{\left(1 - \frac{s_f}{2\,D}\right)^2}{1 - \frac{A_{sl}}{A_g}} \tag{6}$$

and α_{se} and α_{sv} are the coefficients that account for the effectiveness of the steel hoops in the confinement of the concrete along the specimen cross section's plane, and the concrete between steel hoops, respectively [7]:

$$\alpha_{sv} = \frac{\left(1 - \frac{s_s}{2\,d_{st}}\right)^2}{1 - \frac{A_{sl}}{A_g}} \tag{7}$$

For circular columns α_{fe}=α_{ve}=1.0, and for full wrapping configuration α_{fv}=1.0. In Eqs. (6) s_f and D are, respectively, the clear spacing between consecutive FRP strips (for full wrapping s_f=0) and the diameter of the specimen cross section, while s_s and d_{st} of Eq. (7) are, respectively, the steel hoop spacing and the diameter of the steel hoop. In these two equations, A_{sl} is the cross section area of the longitudinal reinforcement and A_g is the area of the specimen cross section.

To obtain values for k_1 of Eq. (2), the results obtained experimentally between k_1=(σ_c-$f_{co,URC}$)/f_l and f_l/$f_{co,URC}$ are plotted in Figure 3. The size of the markers, which was used to distinguish values between the four series of the group of tests, is proportional to ρ_f (see tables 2 and 3).

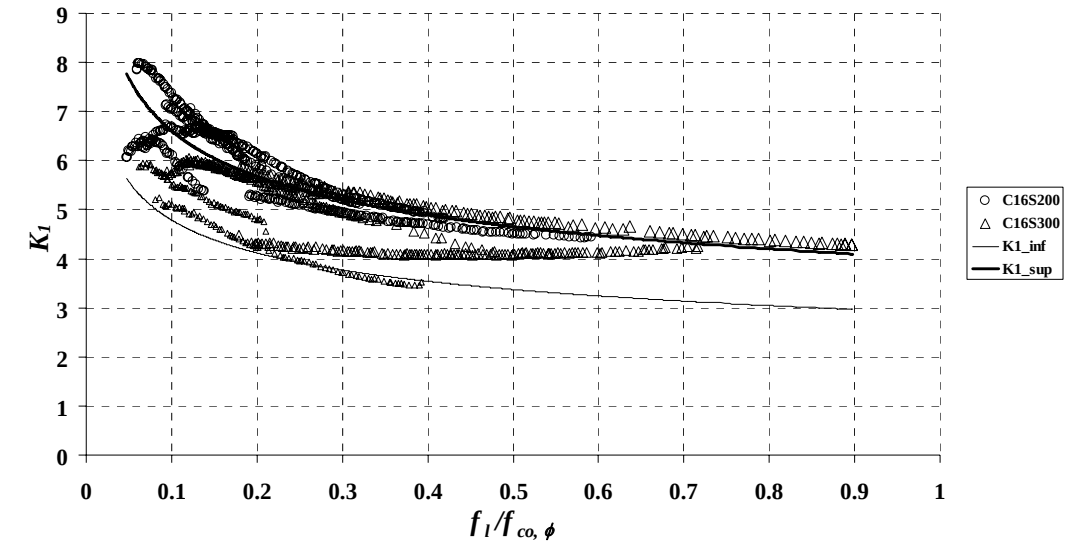

(a)

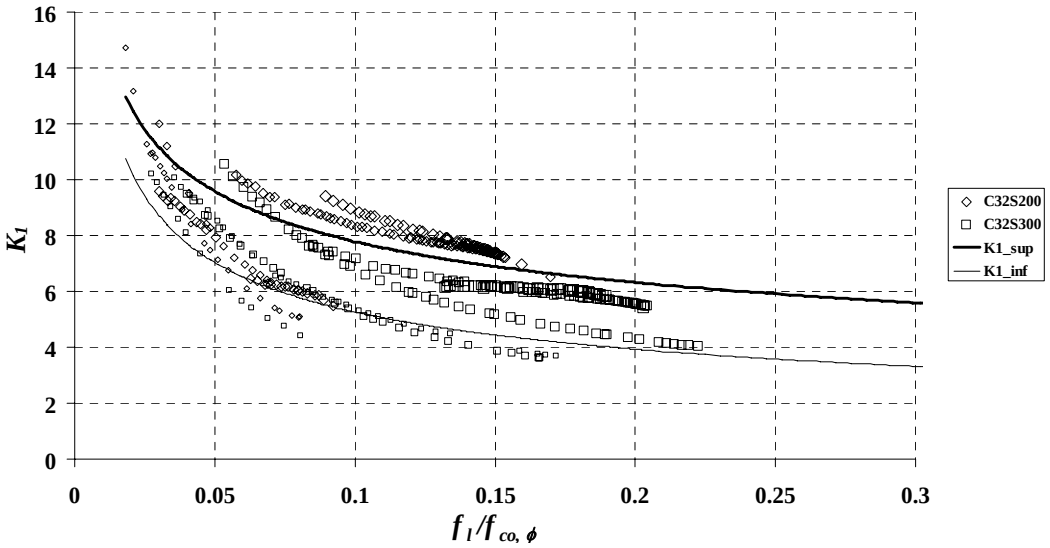

(b)

Figure 3 – Variation of the confinement parameter k_1 with the lateral confining pressure for: (a) C16 and (b) C32 series of tests.

For the C16 and C32 concrete strength levels adopted in the present work (this range is representative of the concrete of structures requiring strengthening intervention) the following equations for k_1 were obtained:

$$k_1 = a\left(\frac{f_l}{f_{co,URC}}\right)^{-b} \tag{8}$$

$a = 2.9 + 72.848\left(\rho_f - 0.0025\right)$; b = 0.2177 for C16 and $\rho_f \in [0.0025; 0.0176]$

$a = 2.0 + 125.828\left(\rho_f - 0.0025\right)$; $b = 0.42 - 7.947\left(\rho_f - 0.0025\right)$ for C32 and $\rho_f \in [0.0025; 0.0176]$

For concrete specimens of $f_{co,URC}$ inside of the strength range of C16 and C32 the k_1 value can be obtained from linear interpolation using the k_1 values determined from (8). $k_{1\text{-sup}}$ and $k_{1\text{-inf}}$ of C16 and C32 concrete strength classes were obtained from Eq. (8) attributing to ρ_f the values 0.0176 and 0.0025, respectively.

To obtain k_2 of Eq. (2), the results registered experimentally between $k_2=(\varepsilon_c/\varepsilon_{co,URC} - 1)/(\sigma_c/f_{co,URC}-1)$ and ε_f are plotted in Figure 4.

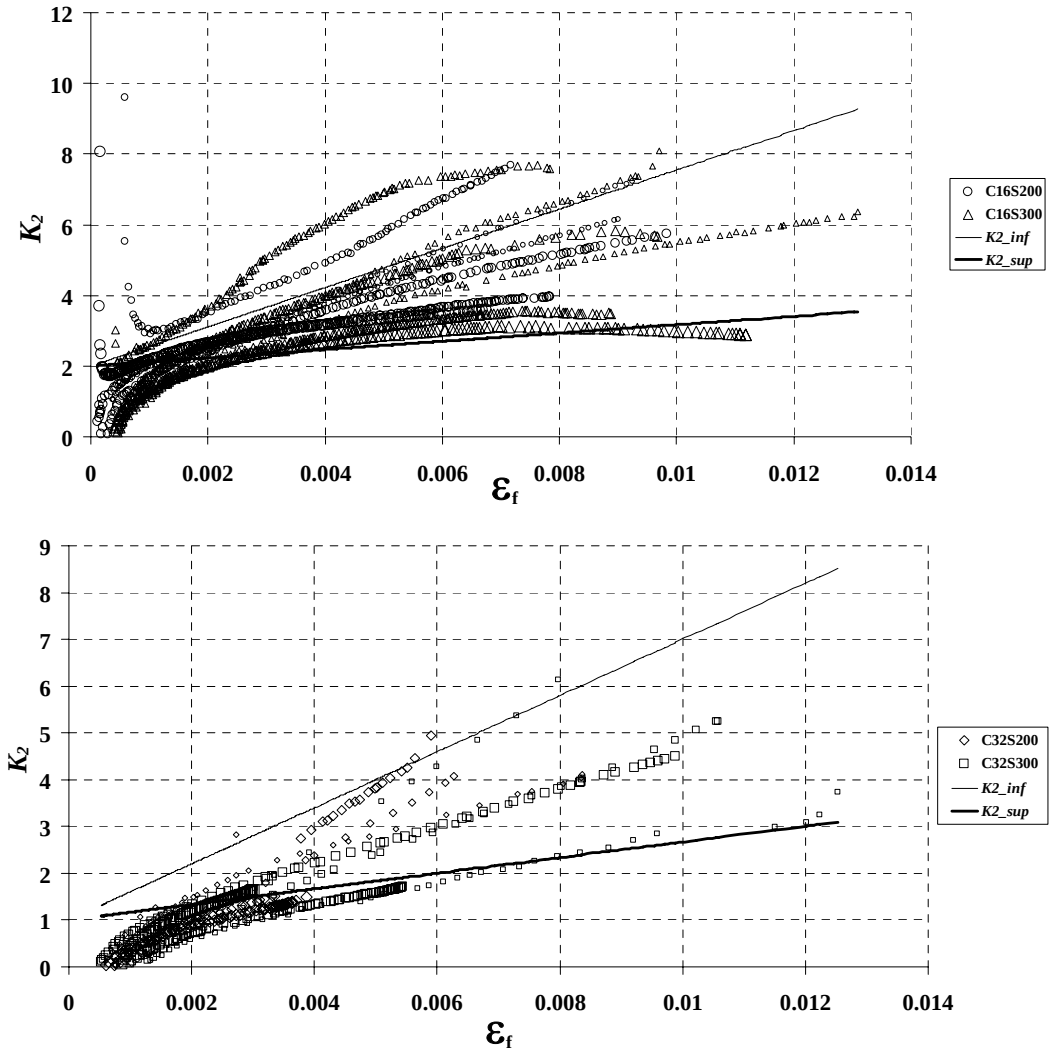

Figure 4 : Variation of the confinement parameter k_2 with the lateral strain.

Based on the obtained results, the following equations were obtained for C16 and C32 concrete strength classes, respectively:

$$k_2 = \left[555 - 29006\left(\rho_f - 0.0025 \right) \right] \varepsilon_f + 2.0 \text{ for C16 and } \rho_f \in [0.0025; 0.0176] \quad (10)$$

$$k_2 = \left[600 - 28695\left(\rho_f - 0.0025 \right) \right] \varepsilon_f + 1.0 \text{ for C32 and } \rho_f \in [0.0025; 0.0176] \quad (11)$$

For concrete specimens of $f_{co,URC}$ within the strength range of C16 and C32 the value of k_2 can be obtained from linear interpolation using the k_2 values determined from (10) and (11).). $K_{2\text{-sup}}$ and $k_{2\text{-inf}}$ of C16 and C32 concrete strength classes were obtained from Eqs. (10) and (11) attributing to ρ_f take the values 0.0176 and 0.0025, respectively.

The model and the experimental stress-strain axial relationships (σ_c-ε_c) are compared in Figure 5. In this figure, compressive strains and stresses are considered as positive values. From the analysis of the represented curves it can be concluded that the developed model is able of predicting, with high accuracy, the axial compression behaviour of CFRP-based confined columns.

The performance of the proposed model was also appraised by simulating the tests carried out by other researchers ([4], [8]). A remarkable agreement between the model and the experimental stress-strain curves is apparent in figure 6. The results predicted by the models proposed by other researcher are also represented in this figure. It can be concluded that the developed model predicted with higher accuracy the experimental results than the predictions of previous models.

5 CONCLUSIONS

The model developed by Harajli et al. to simulate the stress-strain relationship of concrete specimens confined with CFRP was modified in order to be capable of simulating the confinement provided by discrete CFRP-based arrangements. The developed model simulated accurately the stress-strain responses recorded in the experimental program carried out in the ambit of the present work, as well as the tests executed by other researchers.

In comparison to the prediction performance of other available models, the model developed in this study showed higher accuracy on the simulation of CFRP-based confined RC columns of circular cross section.

6 REFERENCES

[1] M., R., Spoelstra and G. Monti, “FRP-confined concrete model”, *J. of composites for construction*, ASCE, 3(3), 143-150, 1999.

[2] H. A., Toutanji and Y. Deng, “Strength and durability performance of concrete axially loaded members confined with AFRP composites sheets”, *J. of Composites*, Elsevier, 255-261, 2001.

[3] Y. Xiao, and H **.**Wu, “Compressive behavior of concrete confined by carbon fiber composite jackets.” *J. of Material in Civil Engineering*, ASCE, 125(3), 255-264, 2000.

[4] L. Lam And J. G. Teng**,** “Design-oriented stress-strain model for FRP-confined concrete.” *J. Construction and Building Materials,* Elsevier, vol. 17, 471-489, 2003.

[5] M. H. Harajli, E. Hantouche And K. Soudki, “Stress-strain model for fiber-reinforced polymer jacketed concrete columns” *ACI Structural Journal,* 105(5), 672-682, 2006.

[6] Ferreira, Débora e Barros, Joaquim (2007). “Comportamento de elementos de pilar confinados com CFRP e submetidos a compressão monotónica”, *Technical report,* March, pp. 294. (http://www.civil.uminho.pt/composites).

[7] Mander, J. B., Priestley, M. J. N. e Park, R. (1988). “Theoretical stress-strain model for confined concrete.” *Journal of Structural Engineering*, ASCE, 114(8), pp. 1804-1826

[8] Triantafillou, T. C.,(2003). Strengthening of Reinforced Concrete Structures with Composite Materials", *Papasotiriou Bookstores*.

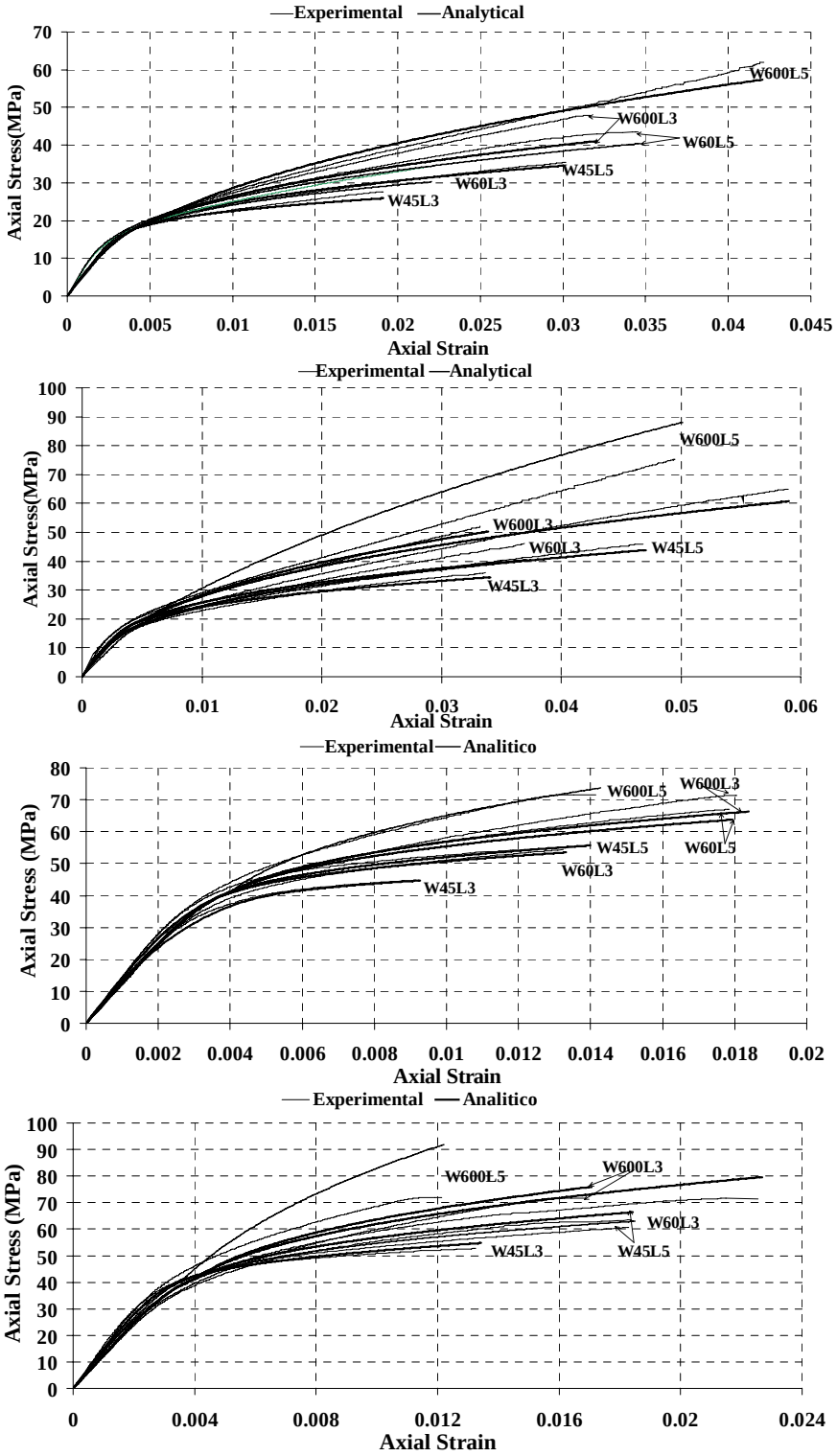

Figure 5: Comparison between the model predictions and the experimental results for the: (a) C16S200ϕ8; (b) C16S300ϕ8; (c) C32S200ϕ8; (d) C32S300ϕ8.

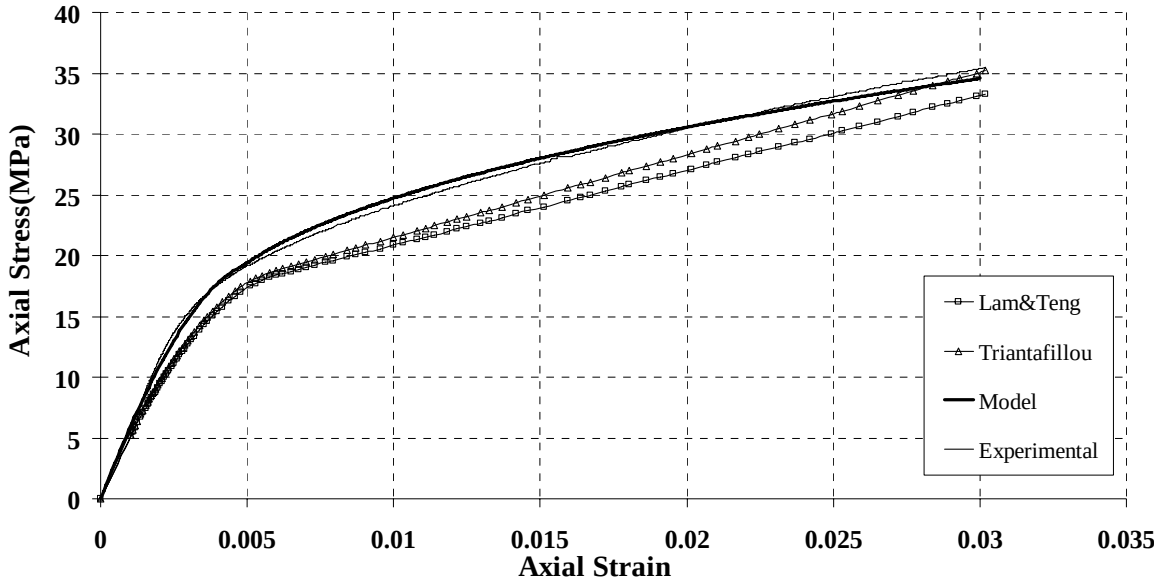

Figure 6: Comparison between the model predictions and the experimental results of Triantafillou and Lam and Teng.